# Investigation of the British pendulum calibration uncertainty by Monte Carlo simulation

To cite this article: V Primoži and M Hiti 2022 *Meas. Sci. Technol.* **33** 015004



OPEN ACCESS
IOP Publishing
Measurement Science and Technology
Meas. Sci. Technol. **33** (2022) 015004 (10pp)
https://doi.org/10.1088/1361-6501/ac2c4b

# Investigation of the British pendulum calibration uncertainty by Monte Carlo simulation

**V Primožič and M Hiti***

Slovenian National Building and Civil Engineering Institute, Dimičeva ulica 12, 1000 Ljubljana, Slovenia

E-mail: miha.hiti@zag.si

Received 17 June 2021, revised 27 September 2021
Accepted for publication 1 October 2021
Published 20 October 2021

**Abstract**

The paper presents the evaluation of the calibration uncertainty of the British pendulum slip resistance tester using Monte Carlo simulation method. A mathematical model was produced which describes pendulum behavior based on its calibration parameters. The Monte Carlo simulation, programmed in Python, was used for simulating the effect of each of the calibration parameters adjustment within their tolerance intervals, with uniform and triangular probability distribution. Four different tolerance limits were compared: limits from a current international standard, a proposition with reduced limits from recent literature, and two novel propositions, one with reduced but easily achievable limits, and a second one for best practically achievable limits. The results of the simulation show a fundamental standard uncertainty contribution of about 2.8% for pendulum calibration according to current standard limits. Furthermore, they suggest a possible improvement to 0.5%–0.7% as its best practical direct calibration standard uncertainty for reduced limits.

Keywords: British pendulum tester, calibration, measurement uncertainty, Monte Carlo simulation

(Some figures may appear in colour only in the online journal)

## 1. Introduction

A British pendulum tester is a simple device for determining slip and skid properties of various surfaces, such as flooring materials, roads, walkways and airstrips. It measures the friction of the test surface by sliding a spring loaded rubber slider mounted at the end of a pendulum arm over a short patch of the test surface. The final indicated value, called British pendulum number (BPN) or pendulum test value, is linked to the energy loss due to the frictional work during the sliding and depends on the pendulum mechanical properties as well as on the slider rubber properties and the test surface itself. The result is indicated on a graduated scale by a drag pointer in contact with the pendulum arm, as the energy loss reduces the final maximum angular position of the pendulum arm at the end of the swing phase, compared to the starting position. Since its development in the 1950s and 1960s it provides a portable and robust test solution for wet and dry slip measurements and is currently included as a standardized device and test procedure in many national and international standards worldwide dealing with prevention of slips and skids. The tester can be easily transported to any location and can be operated by a single person, and at the same time and provides objective results, making it a preferred solution to some other slip testing methods [1, 2].

The British pendulum tester is shown in figure 1. It consists of a stand (A), a rotating pendulum arm (B) with a spring-loaded rubber slider (C), and a measuring scale (D). The arm can rotate freely around its axis. For the measurement, the pendulum arm is released from a horizontal position in order to

* Author to whom any correspondence should be addressed.

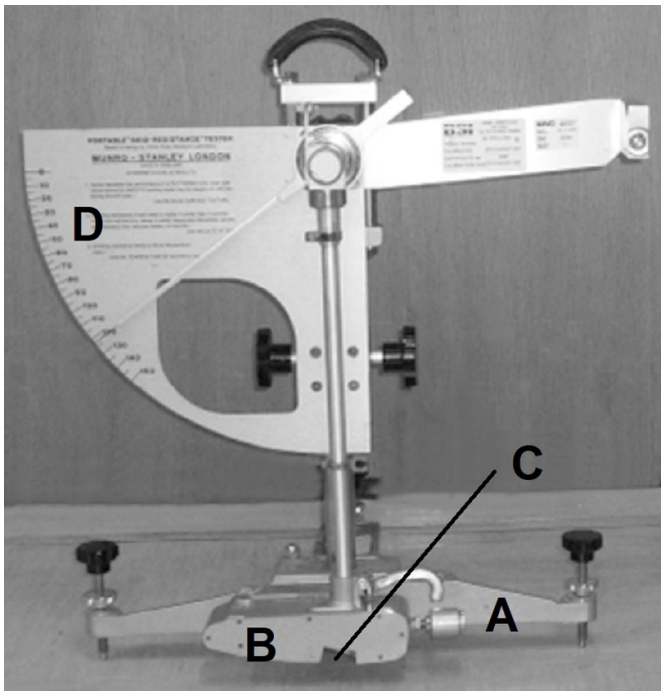


**Figure 1.** British pendulum tester with stand (A) rotating pendulum arm (B), spring-loaded rubber slider (C), and measuring scale (D). Adapted from [3]. 

swing over the test surface. The rubber slider is attached to the pendulum arm end via a spring loaded lever mechanism inside the arm, with the aim to apply an approximately constant force on the test surface during sliding. The pendulum stand is constructed in a way, that it can be easily leveled and the height of the pendulum rotation axis can be adjusted, so that sliding distance matches the defined value. A friction ring is installed at the pendulum axis to adjust the zero BPN reading for a free swing before each test.

The design of the pendulum is defined in several international standards after original design from [4]. Such standards include British standard series BS 7976 [5–7] European standard EN 13036-4 [8], American standard ASTM E303-93 [9], and many others, in which the same device is presented but there can be slight deviations in parameter definition and calibration procedures.

The international standards define the necessary mechanical parameters of the pendulum device and their tolerances to achieve expected performance (informative nominal values for BS 7976 are given):

- the vertical alignment of the stand ($90° \pm 0.5°$),
- the horizontal alignment of the pendulum arm starting point ($0° \pm 0.5°$),
- the length of the pendulum arm from the center of rotation to the edge of the slider ($514 \pm 6$ mm),
- the distance from the center of rotation to the center of mass of the arm ($410 \pm 5$ mm),
- the slider deflection force (nominal $24.5 \pm 1.0$ N with slider force/deflection curve envelope),
- mass of the pendulum arm ($1500 \pm 30$ g),
- the scale offset and graduation ($10 \pm 1$ mm scale drop, scale graduation table),
- mass, dimensions and rubber compound of the slider.

Some of the other defined parameters have little effect on the performance, such as the length (300 mm) and the weight (max. 85 g) of the pointer, and some are indicative only, such as the spring preload force ($22.2 \pm 0.5$ N), as directly setting the actual slider force is much more sensible. The sliding length is set by a marked ruler at the time of the test ($126 \pm 1$ mm). In order to provide reliable results, the device needs to be regularly inspected, adjusted, and calibrated, to make sure its operating parameters are within acceptable limits.

The expected standard deviation of the pendulum test results was shown to be about 5% in recent studies [10], somewhat higher than the 3% from original findings during the development of the pendulum [4]. This is large for applications where slip results provide the basis for safety and health related decisions, as the total expanded uncertainty of the test results reaches or exceeds half of a slip class range (e.g. where the range of a slip class is 10 BPN or less [11]). There are several measurement uncertainty sources influencing the test results dispersion, such as the properties of the test surface, the pendulum rubber properties, operator skill, and environmental conditions, but the fundamental source attributed to the device itself is the the pendulum parameter adjustment. However, there is no available information about what uncertainty to expect from a British pendulum calibrated according to parameter limits given in the standards.

The knowledge of the uncertainty contribution based on the device adjustment is vital to assure long term stability of an individual device and for device-to-device comparability. Furthermore, the device calibration uncertainty and the compliance with the parameter limits provide the basis for setting up the most precise possible pendulum device, which could be used to define reference BPN test values for various slider-surface combination. Some standards already define expected BPN range values for several reference surfaces, such as 3M$^{TM}$ Lapping Film 261X, 3.0 Micron with a range of $\pm 3$ BPN at 61 BPN or $\pm 3$ BPN at 50 BPN (depending on slider rubber type) [8], to check the overall performance of the pendulum, but these values are not consistent across standards and have no appropriate metrological traceability. For comparison, for a similar working principle pendulum device for ductility testing in metal testing—Charpy pendulum test [12]—the standard provides requirements for verification of device parameters (direct calibration) and a requirement for verification of overall performance by performing a test on a reference material (indirect calibration). In this case, the reference value is not generally defined in the standard but a metrologically traceable value is attributed to each set of reference material probes individually with assigned measurement uncertainty based on batch test on a reference Charpy device.

There is ongoing research regarding the the British pendulum performance and its applications in various fields, either for use on different surfaces [13], material characterization [14, 15], its general performance as a measurement instrument

[16–18], new procedures for its calibration [3, 19] with correction of test results for deviant pendulum setups [20–22], and reference surface value determination [22]. However, the uncertainty of the pendulum test result is mostly roughly estimated rather than calculated from the actual pendulum setup and calibration results, and literature on this subject is practically non-existent to the best knowledge of the authors.

The characterization of the measurement uncertainty based on the pendulum model and parameter tolerance limits would confirm the performance of the device and assure necessary metrological traceability of test results, providing improved comparability. The information about the pendulum device uncertainty is also vital to establishing the reference values for reference surfaces, as they are not yet available and are being researched.

In this paper we present the analysis of the measurement uncertainty of the British pendulum calibration based on a developed mathematical pendulum model and Monte Carlo simulation. The uncertainty analysis includes different pendulum parameters constraints, from the estimation of the measurement uncertainty to be expected from established limits in current international standards, to several proposed optimized limits sets to exploit the full metrological potential of the pendulum. The analysis is limited to the effects of the pendulum setup, excluding the effects of slider-surface interaction, other than sliding length and nominal sliding force.

The aims of the paper:

- to develop a mathematical pendulum model,
- to apply Monte Carlo simulation method for uncertainty evaluation,
- to investigate the influence of the device parameters errors on the calibration result,
- to evaluate uncertainty for current parameter limits, based on current standards,
- to evaluate uncertainty for alternative limits from literature,
- to propose and evaluate new limits, including best practical realization.

## 2. Materials and methods

### 2.1. Mathematical model of the apparatus

*2.1.1. Model development.* The schematic representation of the pendulum working principle is shown in figure 2. Pendulum arm with the length $L_s$ from the axis to the slider edge, and its center of mass at distance $L_c$ from the axis, is released from a horizontal position at height $h_1$, shown on the right side, and follows the trajectory shown as a dashed arc on the sketch. When hitting the test surface, the slider has to deflect, reducing $L_s$, to prevent the pendulum arm from coming to a stop, and instead sliding over the surface. The slider deflects for approximately 4.2 mm, and the spring loaded mechanism within the pendulum arm is designed in a way to provide a preload force $F_S$ on the slider in the direction of the pendulum arm. The force $F_S$ rises steeply with the start of deflection and quickly reaches the approximately constant maximum calibrated force $F_C$, producing a frictional force $F_f$ for the duration of the slide

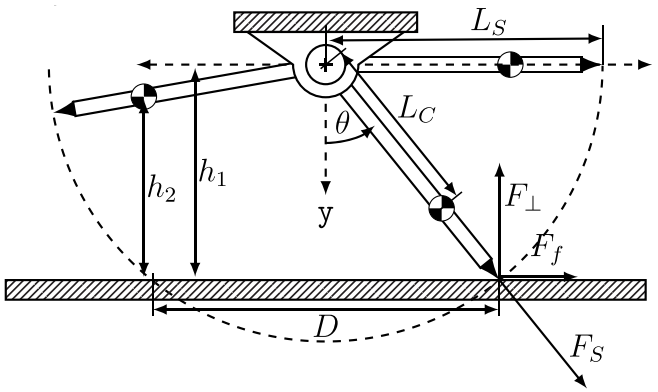


**Figure 2.** Schematic representation of the British pendulum. Start position (right of center) and end position (left of center) of pendulum arm are shown, and the point of contact with the test surface (middle position). Sketch is not in scale and the angles are exaggerated for clarity.

across the test surface over a distance $D$. Due to the energy loss from friction between rubber slider edge and the test surface, the center of mass of the pendulum arm can not reach the same height $h_1$ as at the start of the swing, but a lower final height $h_2$, depending on the amount of friction. The angular position $\theta$ reached by the pendulum at the end of the swing is indicated on an angular scale by a drag pointer.

In constant friction force $F_f$ approximation, the loss of the potential energy $W_g$ depends on the friction force $F_f$ and the sliding distance $D$, therefore the friction coefficient $\mu$ can be expressed as:

$$\mu = \frac{F_f}{F_\perp} = \frac{\Delta W_g}{DF} = \frac{mg(h_1 - h_2)}{DF} \tag{1}$$

where $m$ is the mass of the pendulum arm, $g$ is the gravitational acceleration, $D$ is the sliding distance, $F_\perp$ is the normal force of the slider on the test surface, and $h_1$ and $h_2$ are initial and final position of the center of gravity, respectively. Results of the pendulum measurements are expressed as a BPN. The BPN scale was originally designed to be approximately 100 times the expected friction coefficient $\mu$ [4], based on equation (1), and is given in some standards, e.g. [8].

The pendulum motion model can be obtained from literature [23] as described by equation (2):

$$I\ddot{\theta} + ML_c \sin\theta = F_\perp L_S(\sin\theta + \mu\cos\theta) \tag{2}$$

where $I$ is the moment of inertia, $M$ is the mass of the pendulum arm, $L_C$ is the distance between arm center of gravity and axis of rotation, $L_S$ is the distance between axis of rotation and the slider edge, $F_\perp$ is the normal force on the slider edge, and $\theta$ is the angular displacement of the pendulum arm.

If the torque of the friction ring $M_r$ is included in equation (2), we get equation (3).

$$I\ddot{\theta} + mgL_C \sin\theta - F_\perp L_S(\sin\theta + \mu\cos\theta) - M_r = 0. \tag{3}$$

In [23] approximation for small angles is used, where the force of spring preloaded slider $F_S$ is equal to $F_\perp$. In a general case, the normal force on the test surface depends on the

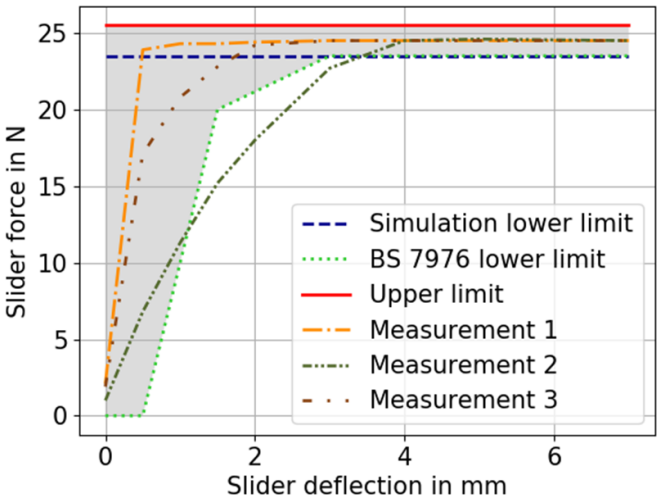


**Figure 3.** Slider force/deflection profile according to BS 7976-3, with shaded expected envelope. For Monte Carlo Method, profile with constant force between 'Simulation lower limit' and Upper limit was used. Measurement 1, 2 and 3 are examples of real force-deflection profiles from [3].

angle of the pendulum arm during sliding ($\theta$ between $\pm 13°$) resulting in equation (4).

$$I\ddot{\theta} + mgL_C \sin\theta - L_S F_S \left( \frac{\sin 2\theta}{2} + \mu \cos^2\theta \right) - M_r = 0. \quad (4)$$

The force $F_S$ from equation (4) differs from 0 only when the slider is in contact with the test surface. In an ideal pendulum, the $F_S$ increases from zero to nominal slider force $F_C$ immediately upon contact, equation (5).

$$F_S(\theta) = \begin{cases} F_C & |\theta| < \arcsin\left(\frac{D/2}{L_S}\right) \\ 0 & \text{else.} \end{cases} \quad (5)$$

*2.1.2. Limitation and constraints of the force model.* In reality, $F_S$ is a function of slider deflection. The force/deflection relation was already studied through experimental analysis and its effects presented in [3]. Examples of real world force/deflection profiles from this work are shown in figure 3, where three measured force profiles are shown, with the shaded part of the envelope according to BS 7976-3. Measurement 1 corresponds to an optimal real world force profile, Measurement 2 is an example of force profile outside of the BS 7976 envelope, and Measurement 3 corresponds to a force profile compliant with the BS 7976 limits and the stricter EN 13036-4 standard. Commercially available pendulum testers in good working order are able to reliably reproduce the profile shown as Measurement 1, reaching the required force plateau within the first 0.5 mm of deflection. Other force profiles, even if inside the envelope, are not representative and are not included within this study—the design of the pendulum expects an approximately constant sliding force throughout the slider deflection.

Furthermore, during the actual pendulum test, the dynamic slider contact force does not exactly follow the static force profile during calibration. Force oscilation and stick-slip phenomena can occur during the sliding [24] with a detailed analysis of the sliding motion using finite element modeling presented in [25, 26]. These dynamic loading effects are not included in the presented uncertainty simulation model as they are not a part of the calibration process.

The original pendulum design should give a linear relation between BPN and coefficient of friction, but it was reported soon after original development in [27] that the actual relation between friction coefficient $\mu$ and the experimental BPN results deviates from linear relation as shown in equation (6),

$$BPN = \frac{330\mu}{3+\mu} \quad (6)$$

and a slider contact force dependency on indicated BPN results was later presented in [28]. As the slider-surface interaction is out of scope of this work, and is therefore not included in the uncertainty model, the uncertainty simulation results were basically linear for BPN-$\mu$ relation, as originally intended, even for different slider deflection/force curves from figure 3. Equation (6) can be used to correct the actual expected test result for slider-surface effects inclusion.

For the Monte Carlo simulation, the slider force $F_C$ was chosen as a constant force between 'Simulation lower limit' and 'Upper limit', corresponding to BS 7976 limits in the constant part of the envelope ($24.5 \pm 1$ N). The piecewise defined function in equation (5) was replaced with a more precise force profile for the simulation of actual measured slider force/deflection characteristic for the validation of the model.

### 2.2. Experimental setup

Equation of motion equation (4) was solved in combination with equation (5), and the solution was compared to the behavior of a real pendulum. A `Python` function `odeint` from package `scipy.integrate` with $10^5$ steps and $1.7 \times 10^4$ s time interval was used. The numerical solution for $\theta(t)$ was calculated for a given set of input parameters for pendulum arm mass $m$, position of center of gravity $L_C$, arm length $L_S$, gravitational acceleration $g$, sliding distance $D$, friction coefficient $\mu$, and initial position of pendulum arm. The zero BPN value was numerically calibrated to determine the needed torque $M_r$ by increasing $M_r$ in steps of 0.02 $Nm$ until the reading of the pendulum was zero within 0.25 BPN. As there is no tolerance limit for the zero reading defined in the standard BS 7976, the interval $\pm 0.25$ BPN was chosen within the indication resolution of the scale.

The output of the developed model was compared to a real pendulum measurement. A high speed 3D camera system with 500 frames per second (Photron Fastcam 1M with GOM Correlate Professional 2016 evaluation software) was used to film the pendulum swing over the reference surface (3M pink lapping film). Points on the pendulum arm and stand were marked with reference marks with three reference points on the pendulum arm, three on the pendulum stand, and one for the pendulum axis, figure 4. Average position of the reference points

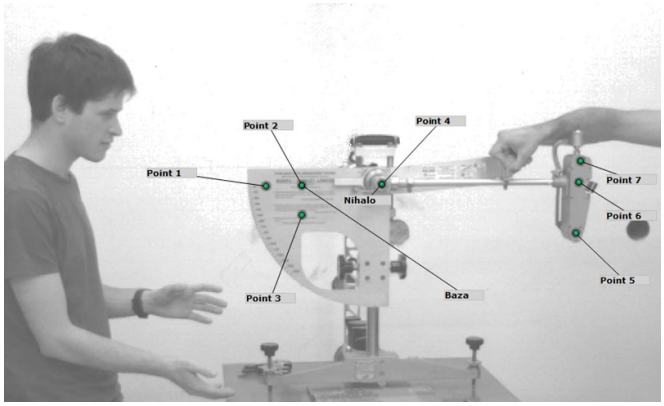


**Figure 4.** Experimental setup: test swing performed over 3M pink lapping film recorded with 3D camera. Reference points marked with stickers are shown.

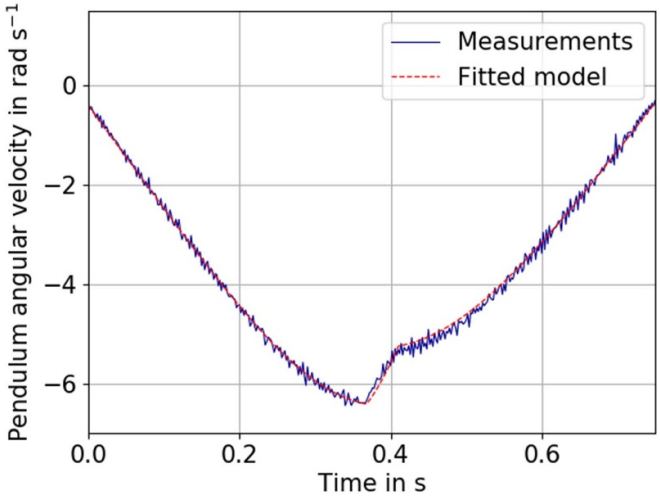


**Figure 5.** Fitted numerical solution of the equation of motion and results of the actual measurement.

on the pendulum arm relative to the reference points on the pendulum stand were used to determine $\theta(t)$.

Model prediction was then fitted to the data with respect to friction coefficient $\mu$ using least squares method and compared to the real measurement, figure 5. The unknown parameters of actual rubber-surface friction coefficient and the dynamic behavior of the sliding force prevent a quantitative assessment of the fit, but it suggests a good agreement within some BPN. Procedure and results were similar to those obtained by [23], although we did not use small angles approximation in equation (4).

### 2.3. Monte Carlo simulation

To conduct the Monte Carlo uncertainty estimation, all important parameters which affect the measurement have to be determined, the physical model has to be produced and the probability density functions (PDFs) of the input parameters need be estimated. Then the Monte Carlo calculations are performed for input parameter values drawn based on their PDFs using an appropriate pseudo-random number generator and the output probability distribution is analyzed.

JCGM 101 method [29] was used with practical applications described in [30]. The simulation was written as a function $f$ of multiple input variables, which returns the theoretically predicted result of the measurement in BPN as the output variable $Y$, equation (7), with the input variables presented in table 1.

$$Y = f(m, L_C, D, L_S, F_S, h, \alpha, \beta, g, \mu). \tag{7}$$

The next step is the determination of the PDF for every variable in the function (7). While according to JCGM 101, a uniform distribution should be used when only lower and upper limit of input quantities are know, a triangular probability distribution would take into account the adjustment not only within the tolerance interval but as close to nominal values as possible during the calibration process. The uncertainty of the pendulum calibration was determined for uniform and triangular probability distribution functions.

Limits for the input variable probability distribution were taken from the tolerance interval limits defined in the standard BS 7976, and also for three different narrower sets of tolerance intervals. One set of narrower tolerances was proposed in [22] (Strautins) and two new sets of tolerance intervals are proposed by the authors for the evaluation: one set of more precise, but also easily achievable tolerance intervals (Proposition A), and a second set with even narrower limits (Proposition B). The latter represent an example of practical limits of real world calibration results, with tolerances about three times the reference equipment calibration uncertainty. The alternative tolerance sets are meant to be used for comparison to standard BS 7976 tolerances to determine the order of magnitude for which the uncertainty could be reduced. Table 1 shows the tolerance interval sets under investigation. For frame levelness, pendulum arm zero position, and scale height, not defined in [22], tolerance intervals from BS 7976 were presumed. The sliding distance $D$ is an integral part of the model, although it can not be adjusted during calibration. A ruler is calibrated and used for setting the sliding length, and the main uncertainty effect arises during measurement set-up.

Random values from within the tolerance interval were drafted. For this, Wichmann–Hill algorithm is proposed in JCGM 101, but we used a more modern Mersenne Twister [31]. We used `Python 3.7.4` [32] with the `scipy 1.3.1` library [33] for numerical integration and random sampling `random` module, which offers sampling of both uniform and triangular probability distributions. Python was chosen as it is freely available and allows both calculation and data processing. However, Monte Carlo method could also be done by other software tools such as Matlab [34] or Microsoft Office Excel [35].

In [30] it is estimated, that Monte Carlo should use $M > \frac{10^4}{1-p}$ samples, for a coverage probability $p$, leading to $M > 200\,000$ for $p = 95\%$. Due to the long computational time, a lower value was selected as $M = 5000$, and justified according to JCGM 101 for smaller $M$ by comparing the simulation results for $M = 500$, $M = 5000$ and $M = 100\,000$ and presuming

**Table 1.** Tolerance intervals for which the uncertainty was determined.

| Parameter | Nominal value | Tolerance interval limits | | | |
|---|---|---|---|---|---|
| | | BS 7976 | Proposition A | Proposition B | Strautins |
| Pendulum mass $m$ | 1500 g | ±30 g | ±5 g | ±1 g | ±10 g |
| Center of gravity position $L_C$ | 410 mm | ±5 mm | ±2 mm | ±1 mm | ±3 mm |
| Sliding distance $D$ | 126 mm | ±1 mm | ±1 mm | ±1 mm | ±1 mm |
| Pendulum length $L_S$ | 514 mm | ±6 mm | ±1 mm | ±1 mm | ±1 mm |
| Nominal slider force $F_S$ | 24.5 N | ±1.0 N | ±0.25 N | ±0.1 N | ±0.3 N |
| Scale height $h$ | −10 mm | ±1 mm | ±1 mm | ±1 mm | ±1 mm[a] |
| Stand tilt $\alpha$ | 90° | ±0.5° | ±0.5° | ±0.2° | ±0.5°[a] |
| Initial position tilt $\beta$ | 0° | ±0.5° | ±0.5° | ±0.2° | ±0.5°[a] |

[a] Data from BS 7976.

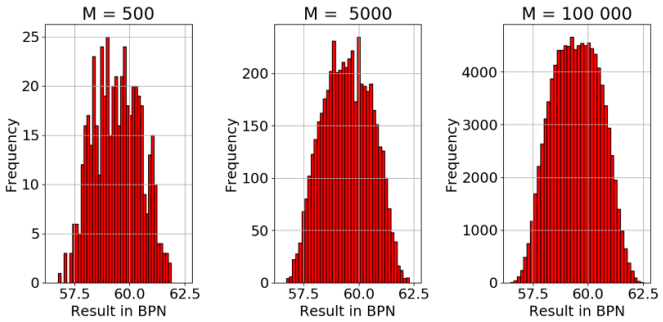


**Figure 6.** Distributions of output variable for different numbers of samples. 5000 samples per $\mu$ were chosen as the smallest number, where the quantity of samples was not affecting measured $\sigma$. Output PDF was found out to be normal using Kolmogorov–Smirnov test with $p = 9.9 \times 10^{-6}$.

a normal output distribution. As shown in figure 6, higher values of $M$ produced more coherent distribution, but the difference between $M = 5000$ and higher values of $M$ did not affect the standard deviation significantly. The output PDF for $M = 5000$ was additional confirmed to be normal by Kolmogorov–Smirnov test of the fitted normal distribution with $p = 9.9 \times 10^{-6}$. Test was made with Python library `scipy.stats`.

Monte Carlo method was used to assess uncertainty for chosen $\mu$ in the range from 0 to 1.5 in 0.05 steps. The simulation procedure is presented in figure 7. For a selected $\mu$, random samples are first drawn for input parameters from their defined PDFs. The pendulum differential equation is then solved for $\mu = 0$ within a loop with varying $M_r$ until the output value of the simulation result is 0 BPN (within ±0.25 BPN) to set the friction ring effect for zero indication. This is followed by the actual calculation of the differential equation output for the selected $\mu$, with the calculation of the BPN result from the maximum amplitude of the pendulum angle. This procedure is repeated $N = 5000$ times for each input $\mu$. After the completion of Monte Carlo calculations, the standard deviation of the output is calculated as the uncertainty estimate.

The computational time for the simulation was approximately 55 h on Intel Core i7 processor (7th generation) laptop, mostly due to the inefficient friction ring adjustment routine taking approximately 90% of the computational time. The

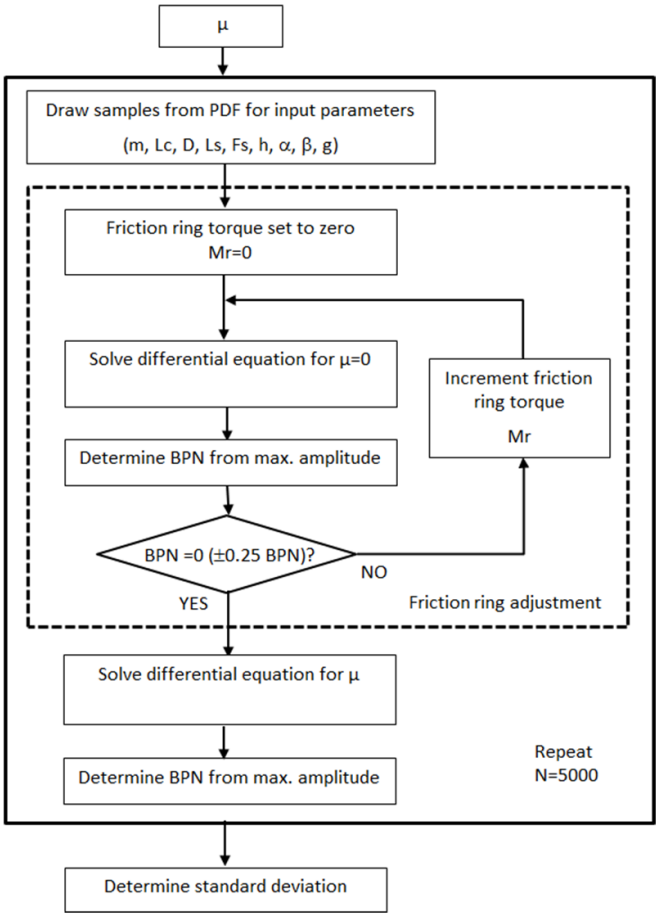


**Figure 7.** Flowchart for the Monte Carlo simulation.

friction ring adjustment, however, is key to correct simulation results, as most influence parameters depend on reliable zero BPN adjustment. The procedure could be improved in the future to reduce the computational time for example by interpolation of the input friction ring values.

### *2.4. GUM uncertainty evaluation*

The mathematical model of the pendulum also gave the possibility to estimate the sensitivity of the result to each parameter deviation. Each parameter was set to maximum

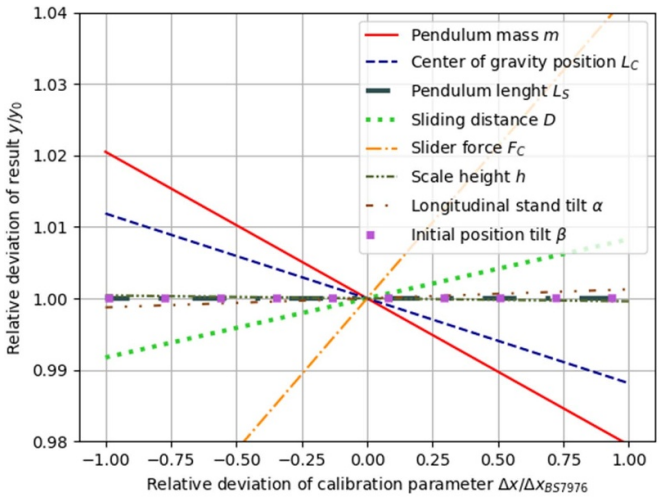


**Figure 8.** The impact of changing one variable, when the others are fixed to nominal value. Graph is plotted for $\mu = 0.6$. The relative deviation of variable from nominal value as $\Delta x/\Delta x_{BS7976}$, where $\Delta x_{BS7976}$ is width of tolerance interval form table 1 is plotted on $x$-axis for BS 7976 tolerance limits.

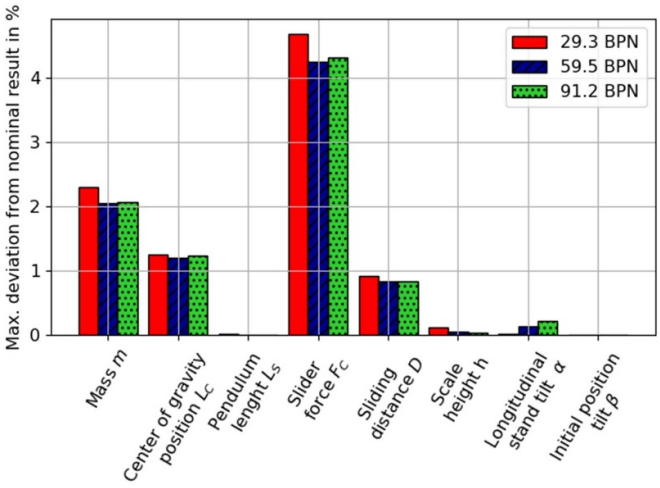


**Figure 9.** Maximum deviation for result $Y$ for one parameter at maximum limit and other parameters at nominal values. Results for $\mu = 0.3$, $\mu = 0.6$, $\mu = 0.9$ shown in BPN. BS 7976 tolerance limits.

allowed deviation with all other parameters fixed at nominal values. Figure 8 shows the result for $\mu = 0.6$ for each of the calibrated parameters within BS 7976 limits. It can be observed, that the input variables have different effects on the output result, with the most critical being the slider force, followed by pendulum arm mass, pendulum arm center of gravity position, and the sliding distance. It can also be seen that most parameters seem to have a quite linear relation, which would justify the use of LPU to calculate uncertainty, if partial derivatives of function in equation (7) would be numerically calculated. Figure 9 shows maximum expected deviations for result $Y$ based on each parameter contribution for $\mu = 0.3$, $\mu = 0.6$, and $\mu = 0.9$ friction coefficients.

Based on the data from figures 8 and 9, the contribution for each uncertainty component can be estimated as a standard uncertainty from its maximum influence and expected probability distributions, and a combined standard uncertainty can be expressed as given by equation (8):

$$u_c(Y)^2 = u(m)^2 + u(L_c)^2 + u(D)^2 + u(L_s)^2 + u(F_s)^2 + u(h)^2 + u(\alpha)^2 + u(\beta)^2 + u(g)^2 + u(\mu)^2. \quad (8)$$

## 3. Results and discussion

The results of the Monte Carlo simulation based on the pendulum model for limit sets from table 1 are shown in table 2. Uncertainty for $\mu$ in the range from 0 to 1.6 with 0.05 step was determined for uniform and triangular probability distribution for each limit set. Results are shown for BPN values for the range 20–160 BPN with uncertainties expressed in units of BPN as expanded uncertainties (for $k = 2$). As expected, the uncertainty decreases with reduced limits and it is increasing with the result of the test.

When expressed as relative uncertainty $U/Y$, the result is shown in figure 10 for uniform probability distribution and in figure 11 for triangular probability distribution. Relative uncertainty increases sharply with low BPN values below 30 and there is a slow increase for higher BPN values. The relative uncertainty is high for small BPN values mostly due to high impact of the friction ring setting resolution.

For a pendulum calibrated according to BS 7976, the uncertainty determined with the Monte Carlo simulation with uniform probability distribution of input parameters has a minimum at about 30 BPN, where the expanded uncertainty is about 5.2%. As can be seen in the figure 10, the expanded uncertainty is under 5.5% for BPN values in the range from about 15 BPN–75 BPN. Expanded uncertainty is within 6.5% for the whole range. This value is lower than the value reported in practical comparisons of pendulum test results [10], where additional uncertainty contributions are included (slider-surface interactions, operator skill, etc).

Limit set Strautins assures expanded uncertainties between 2.0% and 3.0% for BPN values above 10. Limit set Proposition A results in expanded uncertainty between 1.7% and 2.5% while Proposition B results in expanded uncertainty values between 1.2% and 2.0% for most of the range. All three propositions significantly improve the performance of the pendulum compared to the limits from BS 7976 standard.

These results agree quite good with the expanded uncertainty calculated according to GUM following equation (8), with results for $\mu = 0.6$ giving $U = 5.6\%$ for BS 7976, $U = 1.7\%$ for Proposition A, $U = 1.2\%$ for Proposition B, and $U = 2.1\%$ for limit set Strautins.

Expanded uncertainty determined by Monte Carlo simulation with triangular probability distribution of input parameters further lowered the uncertainty as shown in figure 11. The BS 7976 limits result in expanded uncertainty of about 4.0% for the critical range from 20 BPN to 100 BPN and mostly below 5.0% for the whole range. Proposition Strautins results in expanded uncertainty below 2.0% for the most part of the range. Proposition A results in expanded uncertainty slightly lower than proposition Strautins and is below 1.5% from 20

**Table 2.** Expanded calibration uncertainty $U$ ($k = 2$) determined for different BPN results for four different sets of tolerance intervals for uniform and triangular PDFs.

| BPN Value | | 19.8 | 39.5 | 60.2 | 80.7 | 104.4 | 129.1 | 157.2 |
|---|---|---|---|---|---|---|---|---|
| BS 7976-3 | Uniform PDF | 1.02 | 2.04 | 4.41 | 4.36 | 5.89 | 7.72 | 10.01 |
| | Triangular PDF | 0.78 | 1.54 | 2.40 | 3.23 | 4.38 | 5.66 | 7.47 |
| Proposition A | Uniform PDF | 0.37 | 0.67 | 1.05 | 1.49 | 2.00 | 2.67 | 3.47 |
| | Triangular PDF | 0.29 | 0.51 | 0.76 | 1.06 | 1.53 | 1.90 | 2.61 |
| Proposition B | Uniform PDF | 0.28 | 0.47 | 0.69 | 0.97 | 1.29 | 1.72 | 2.36 |
| | Triangular PDF | 0.23 | 0.36 | 0.51 | 0.70 | 0.92 | 1.21 | 1.66 |
| Strautins | Uniform PDF | 0.44 | 0.85 | 1.3 | 1.83 | 2.43 | 3.32 | 4.51 |
| | Triangular PDF | 0.34 | 0.61 | 0.95 | 1.29 | 1.73 | 2.34 | 3.14 |

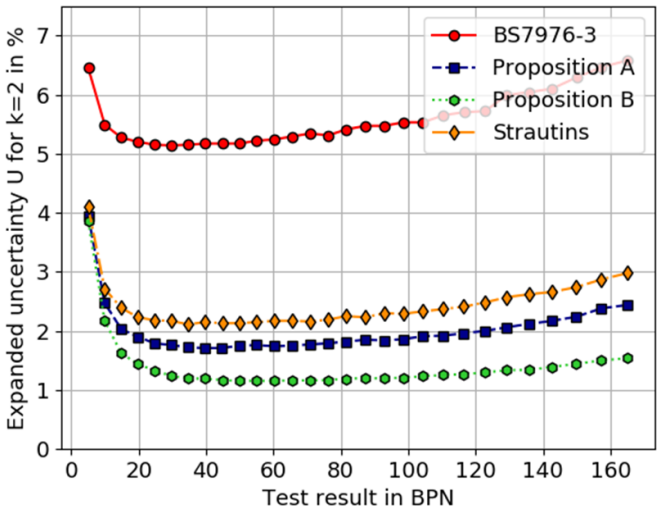


**Figure 10.** Uncertainty of British pendulum calibration when uniform probability distribution function is presumed for all input variables. Relative expanded uncertainty is shown.

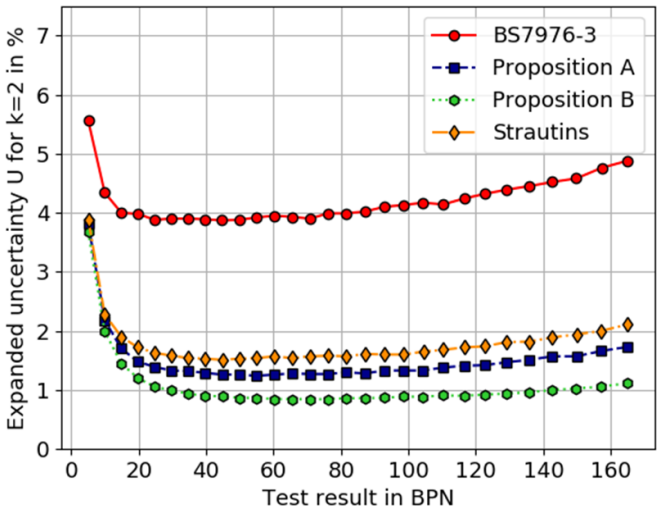


**Figure 11.** Uncertainty of British pendulum calibration when triangular probability distribution function is presumed for all input variables. Relative expanded uncertainty is shown.

BPN to 100 BPN. Proposition B further reduces the uncertainty to mostly to 1.2% and below.

The presented results can be directly employed for evaluation of measurement uncertainty of British pendulum test results if the Pendulum meets the requirements of the evaluated limit sets. In these cases, the British pendulum test result standard uncertainty $u$ can be calculated following equation (9), where the uncertainty contribution from the pendulum design calculated by Monte Carlo simulation $u_{MC}$, is combined [36] with the zero setting resolution $u_{res\_zero}$, indication resolution of the pendulum device $u_{res\_ind}$, and the standard deviation due to repeatability of the test $u_{stdev}$.

$$u = \sqrt{(u_{MC}^2 + u_{res\_zero}^2 + u_{res\_ind}^2 + u_{stdev}^2)}. \tag{9}$$

For a surface-slider combination indicating 60 BPN and a good repeatability of the test ($u_{stdev} = 0$ at indication resolution of 1 BPN and 0.5 BPN zero setting resolution), the expected best expanded uncertainty of a general pendulum device within the standard limits (BS 7976) would be about 5.7% or 3.7 BPN. For a carefully adjusted pendulum and following the limits from proposition B this would be reduced to about 1.28% or 0.84 BPN.

Proposition B would in this case allow characterization of a reference surface with values of around 60 BPN, such as the 3M lapping film, with expanded uncertainty around 0.9 BPN. This could in turn lead to indirect calibration of the British pendulum tester with the expanded uncertainty of about 1.1 BPN.

Following the analogy with international standards for Charpy pendulum [12], standards defining the British pendulum and test method could be revised to include direct and indirect calibration methods and provide reference values for standard slider-surface combinations. This would lead to the significant improvement of the comparability of the British pendulum devices and their test results.

## 4. Conclusion

The paper presented the evaluation of the British pendulum calibration measurement uncertainty using Monte Carlo simulation for standard tolerance limits and additional optimized limits. A mathematical model of the British pendulum was proposed and Monte Carlo simulation was successfully performed in `Python` scripting language. The results give the estimation of the fundamental calibration uncertainty stemming from the calibration parameter tolerances.

Based on the pendulum model, the parameters with the major effect on the final measurement uncertainty of the calibration were identified. Care should be taken to reduce the deviation of these parameters during calibration and also during each test set-up.

The simulation for the calibration uncertainty evaluation included four different tolerance sets for the calibrated parameters, including two newly proposed tighter limit sets, with uniform and triangular probability distribution of input parameters for comparison. The expected standard uncertainty of a pendulum calibration according to current standard limits amounts to about 2.8% from the calibration tolerances alone. These results are directly applicable to evaluation of pendulum test uncertainty as they providing the fundamental uncertainty contribution.

The results of all three alternative calibration limit sets suggest a possible improvement of the pendulum performance by at a factor of 3–5. The two newly proposed limits would improve the standard uncertainty of the British pendulum calibration to values below 0.7% in the critical range, with the possibility of reaching values below 0.5%.

For British pendulum testers calibrated within the parameter limits discussed in the paper, the users can work with the presented calibration uncertainty and expand it by including additional components specific to their test setup, e.g. force/deflection curve deviation contribution, and slider rubber and test surface properties contributions. Pendulum testers calibrated to tighter tolerance limits can furthermore provide a reference standard for characterization of reference surfaces, in the next step allowing an indirect calibration of typical pendulum testers of end-users by these newly defined reference surfaces values. The result offer a possibility to amend the international standard across the application field of the British pendulum for improved performance of the test method.

## Data availability statement

The data that support the findings of this study are available upon reasonable request from the authors.

## Acknowledgments

The authors acknowledge the financial support from the Slovenian Research Agency (Research Core Funding No. P2-0273).

The authors would like to thank Uroš Ristić and Vladimir Požonec from ZAG Department of structures—Laboratory for Structures for providing and operating the optical 3D acquisition system, and Vilma Ducman and Roman Maček from ZAG Department of materials—Laboratory for Cements, Mortars and Ceramics for providing and operating the British pendulum tester.

The authors would like to thank members of UK Slip Resistance Group and Slip Resistance Group Spain for organizing and performing a comparison of British pendulum tester performance in Madrid in November 2018 which lead to the presented work.

## ORCID iD

M Hiti https://orcid.org/0000-0002-5291-7342

## References

[1] Ricotti R, Delucchi M and Cerisola G 2009 A comparison of results from portable and laboratory floor slipperiness testers *Int. J. Ind. Ergon.* **39** 353–7

[2] Mataei B, Zakeri H, Zahedi M and Nejad F 2016 Pavement friction and skid resistance measurement methods: a literature review *Open J. Civil Eng.* **6** 537–65

[3] Hiti M and Ducman V 2014 Analysis of the slider force calibration procedure for the British pendulum skid resistance tester *Meas. Sci. Technol.* **25** 025013

[4] Giles C G, Sabey B E and Cardew K H 1962 Development and performance of skid resistance test *Symp. on Skid Resistance* (West Conshohocken, PA: ASTM International) pp 50–74

[5] BS 7976-1:2002+A1:2013 2002 *Pendulum Testers. Specification* (London: British Standard Institution (BSI))

[6] BS 7976-2:2002+A1:2013 2002 *Pendulum Testers. Method of Operation* (London: British Standard Institution (BSI))

[7] BS 7976-3:2002+A1:2013 2002 *Pendulum Testers. Method of Calibration* (London: British Standard Institution (BSI))

[8] EN 13036-4:2011 2011 *Road and Airfield Surface Characteristics—Test Methods—Part 4: Method for Measurement of Slip/Skid Resistance of a Surface: The Pendulum Test*

[9] ASTM E303-93(2018) 2018 *Standard Test Method for Measuring Surface Frictional Properties Using the British Pendulum Tester* (West Conshohocken, PA: ASTM International)

[10] Goubert L 2006 *Report of the Second Round Robin Test for SRT Pendulums and Other Skidding Resistance Measuring Devices* (Bergisch-Gladbach: BAST) pp 22–23

[11] Bowman R 2010 Slip resistance testing—zones of uncertainty *Bol. Soc. Esp. Ceram. Vidrio* **49** 227–38

[12] ISO 148-2 2016 *Metallic Materials—Charpy Pendulum Impact Test—Part 2: Verification of Testing Machines* (International Organisation for Standardization)

[13] Karaca Z, Gürcan S, Gökçe M V and Sivrikaya O 2013 Assessment of the results of the pendulum friction tester (EN 14231) for natural building stones used as floor-coverings *Constr. Build. Mater.* **47** 1182–7

[14] Wang H, Wang C, Bu Y, You Z, Yang X and Oeser M 2020 Correlate aggregate angularity characteristics to the skid resistance of asphalt pavement based on image analysis technology *Constr. Build. Mater.* **242** 118150

[15] Khasawneh M A and Alsheyab M A 2020 Effect of nominal maximum aggregate size and aggregate gradation on the surface frictional properties of hot mix asphalt mixtures *Constr. Build. Mater.* **244** 118355

[16] Genovese A, D'Angelo G A, Sakhnevych A Farroni F 2020 Review on friction and wear test rigs: an overview on the state of the art in tyre tread friction evaluation *Lubricants* **8** 91

[17] Zaid N B M *et al* 2019 Evaluation of skid resistance performance using British pendulum and grip tester *IOP Conf. Ser.: Earth Environ. Sci.* **220** 012016

[18] Alhasan A, Smadi O, Bou-Saab G, Hernandez N and Cochran E 2018 Pavement friction modeling using texture measurements and pendulum skid tester *Transp. Res. Rec.* **2672** 440–51

[19] Guo W, Chu L and Fwa T 2020 Evaluation of calibration procedures of British pendulum tester *J. Test. Eval.* **49** 1729–46
[20] Guo W, Chu L and Fwa T F 2021 Mechanistic harmonization of British pendulum test measurements *Measurement* **182** 109618
[21] Chu L, Guo W and Fwa T F 2020 Theoretical and practical engineering significance of British pendulum test *Int. J. Pavement Eng.* 1–8
[22] Strautins C 2020 Pendulum calibration, metrological traceability and reference material *Slips, trips & falls Conf. Madrid 2020: "A visions for the future" Int. Slips Trips and Falls Conf.* (*Madrid*, *13–14 February 2020*)
[23] Kulakowski B T, Henry J J and Lin C 1990 A closed-loop calibration procedure for British pendulum test *Surface Characteristics of Roadways: Int. Research and Technologies* (West Conshohocken, PA: ASTM International) pp 103–12
[24] Andrew K R and Cunningham A 1998 Measurement of energy loss profiles during short duration sliding contacts: a computer-compatible instrument based on the British pendulum skid tester *Meas. Sci. Technol.* **9** 1566–70
[25] Liu Y, Fwa T F and Choo Y S 2003 Finite-element modeling of skid resistance test *J. Transp. Eng.* **129** 316–21
[26] Kelvin L Y P 2004 Analyzing laboratory skid resistance test using finite element modeling *PhD Thesis* Department of Civil Engineering, National University of Singapore
[27] Sabey B E and Lupton G N 1964 Friction on weat surfaces of tre-tread-type vulcanizates *Rubber Chem. Technol.* **37** 878–93
[28] Grönqvist R, Hirvonen M and Tohv A 2000 Evaluation of three portable floor slipperiness testers *Int. J. Ind. Ergon.* **25** 85–95
[29] JCGM 101:2008 2008 *Evaluation of Measurement Data—Supplement 1 to the 'Guide to the Expression of Uncertainty in Measurement'—Propagation of Distributions Using a Monte Carlo Method*
[30] Couto P R G, Damasceno J C and de Oliveira S P 2013 Monte Carlo simulations applied to uncertainty in measurement *Theory and Applications of Monte Carlo Simulations* ed W K Chan (eBook: IntechOpen) pp 27–51
[31] Eddelbuettel D 2007 Soft versus hard: a comparison of random number generators between R, GSL and a non-deterministic generator (available at: www.stat.auckland.ac.nz/dsc-2007/abstracts/eddelbuettel06Oct16.pdf)
[32] Python Software Foundation Python Language Reference (Version 3.7) *Python* (available at: www.python.org)
[33] Virtanen P *et al* 2020 SciPy 1.0: fundamental algorithms for scientific computing in Python *Nat. Methods* **17** 261–72
[34] Jie H, Huaiyan C and Yun C 2011 Uncertainty evaluation using Monte Carlo method with MATLAB *10th Int. Conf. Electronic Measurement & Instruments ICEMI'2011* pp 282–6
[35] Chew G, Walczyk T and Monte A 2012 Carlo approach for estimating measurement uncertainty using standard spreadsheet software *Anal. Bioanal. Chem.* **402** 2463–9
[36] JCGM 100:2008 2008 *Evaluation of Measurement Data—Guide to the Expression of Uncertainty in Measurement*